

Effects of crystallinity and crosslinking on the thermal and rheological properties of ethylene vinyl acetate copolymer

Y.T. Sung^a, C.K. Kum^{a,b}, H.S. Lee^b, J.S. Kim^a, H.G. Yoon^c, W.N. Kim^{a,*}

^a Department of Chemical and Biological Engineering, Applied Rheology Center, Korea University, Anam-dong, Seoul 136-701, South Korea

^b Tech. Center, LG Chemical Ltd, 84, Jang-dong, Yusong-ku, Daejeon 305-343, South Korea

^c Department of Materials Science, Korea University, Seoul, South Korea

Received 5 January 2005; accepted 28 September 2005

Available online 21 October 2005

Abstract

Effects of crosslinking and crystallinity on the properties of the thermal and rheological properties of the EVA were studied. From the studies of storage modulus of the EVA with VA content in the solid temperature range (about -70 to 50 °C), the storage modulus decreased with increasing the VA content. This result suggested that the crystallinity of the EVA affected the storage modulus of the EVA because of the weak crosslinking of the EVA by DCP. From the studies of complex viscosity of the EVA with and without DCP in the melt state, the values of the power law parameter of the EVA without DCP ranged from 0.39 to 0.50 and the EVA with DCP ranged from 0.03 to 0.12. In the measurement of the complex viscosity of the EVA in the melt state, the crosslinking affected the complex viscosity of the EVA with DCP.

© 2005 Elsevier Ltd. All rights reserved.

Keywords: Ethylene vinyl acetate copolymer; Crystallinity; Crosslinking

1. Introduction

Ethylene vinyl acetate copolymer (EVA) is a random copolymer consists of ethylene and vinyl acetate (VA) as a repeating unit. The EVA shows various properties with varying the VA content. The properties of the EVA are caused by the crystallinity of the EVA [1–4] which can be controlled by the VA content. The crystallinity of the EVA with the VA content is very important to understand the thermal and rheological properties of the EVA. Many researches have been studied the crystallinity of the EVA. For example, Brogly et al. [1] and Arzac et al. [2] have investigated the effects of crystallinity on the thermal properties of the EVA with VA content.

In some cases, the EVA is required high melt strength in the processing such as foaming. The high melt strength can be achieved by crosslinking the EVA with the dicumyl peroxide (DCP). The crosslinking of the EVA by DCP is caused by the formation of the radical of the DCP.

The EVA could be used as an artificial leather. When the EVA is used as an artificial leather, the flexibility, which is

related to the modulus and crystallinity of the EVA, is an important property. Also, the complex viscosity of the EVA is related to the melt strength during the processing in the melt state of the EVA. In this study, we have investigated the crystallinity and crosslinking behavior of the EVA by varying the VA content from 26 to 46 wt%. To characterize the EVA samples, dynamic mechanical thermal analyzer (DMTA) and X-ray diffractometer were used to measure the dynamic mechanical behavior and morphology of the EVA, respectively. Complex viscosity of the EVA was measured by the advanced rheometric expansion system (ARES) with dynamic frequency sweep mode.

2. Experimental

2.1. Sample preparations

The EVAs used in this study were obtained from commercial sources. The properties of the EVAs by varying the VA content from 26 to 46 wt% are summarized in Table 1. In Table 1, EVA 26, 33, 41, and 46 represent the EVA containing the 26, 33, 41, and 46 wt% vinyl acetate in the EVA. The mixture of the EVA and DCP were prepared by melt extrusion. The DCP, ranging from 0 to 2.0 wt% (phr) with respect to the weight fraction of the EVA were used. The crosslinking of the EVA by DCP has been reported by other

* Corresponding author. Tel.: +82 2 3290 3296; fax: +82 2 924 1793.

E-mail address: kimwn@korea.ac.kr (W.N. Kim).

Table 1
Characteristics of ethylene vinyl acetate copolymer (EVA) used in this study

Samples	VA content (wt%)	T_g (°C) ^a	Melt index (g/min) ^b
EVA 26 ^c	26.0	−16.0	3.0
EVA 33 ^d	33.0	−16.0	15
EVA 41 ^d	41.0	−16.0	2.0
EVA 46 ^d	46.0	−16.0	2.5

^a Measured in our laboratory by DMTA.

^b Measured by ASTM D 1238 (190 °C and 2.16 kg).

^c Supplied by Hanwha Chem. Co.

^d Supplied by Dupont-Mitsui Polychem. Co.

researchers [5]. The temperature of the extruder was set at 85 and 100 °C in feeding and barrel zones, respectively. Samples were compression molded using a hot press at 130 °C for 5 min. For the DMTA and X-ray diffraction tests, crosslinked samples were prepared by the DCP using a hot press at 220 °C for 10 min.

2.2. Dynamic mechanical thermal analysis (DMTA)

DMTA measurements were carried out on advanced rheometric expansion system (ARES) in oscillatory torsional mode at 0.1% strain and 1 Hz frequency. The temperature was scanned from −100 to 100 °C at a rate of 5 °C/min.

2.3. X-ray diffraction analysis

X-ray diffraction pattern measurements were carried out on Mac Science, MXP-HF. The accelerating voltage was 40 kV and the current was 100 mA. The scanning range was 1.8–40° with a scanning rate of 1°/min.

2.4. Rheological measurements

Rheological measurements were carried out on ARES in oscillatory shear at 5% strain in the parallel-plate arrangement with 25 mm plate under dry nitrogen atmosphere. The samples used in this test were fabricated in a disk with 2 mm in thickness. The frequency sweeps from 0.05 to 100 rad/s were carried out at 130 °C. For the rheological measurements, the crosslinked samples were prepared at 220 °C and for 10 min before the dynamic frequency sweep test.

3. Results and discussion

3.1. Effects of crosslinking

Fig. 1 shows the loss factor ($\tan \delta$) vs temperature for the EVA 26 with DCP content. For the EVA 26 with 0, 0.5, 1.0, 1.5, and 2.0 phr DCP, the maximum $\tan \delta$ peak is observed at −16 °C and the maximum peak of the EVA 26 does not change with the DCP content. For the EVA 26 with 0 phr DCP, the $\tan \delta$ shoulder is observed between 0 and 30 °C, which might be the rigid amorphous fraction. The rigid amorphous fraction represents the portion of the amorphous phase remains rigid

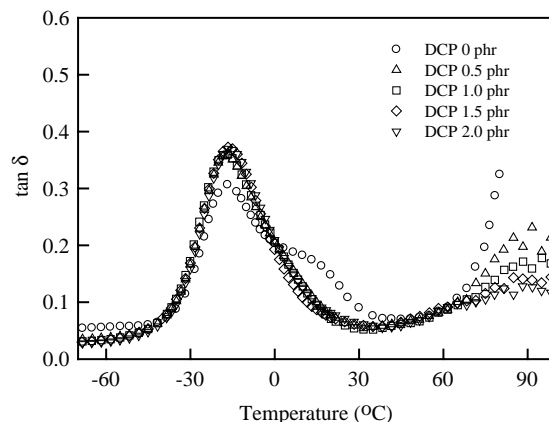


Fig. 1. Loss factor ($\tan \delta$) vs temperature for the EVA 26 with DCP content: (○) 0 phr DCP; (△) 0.5 phr DCP; (□) 1.0 phr DCP; (◇) 1.5 phr DCP; (▽) 2.0 phr DCP.

above glass transition temperature (T_g) [6,7]. By increasing the DCP content in the EVA 26, the $\tan \delta$ shoulder is not observed.

The intensity of the $\tan \delta$ peak is used for the quantitative analysis of the amorphous phase of the polymer [8]. For example, Tsagaropoulos and Eisenberg [8] have reported the area of the $\tan \delta$ peak in the study of the polymer/silica composite. From Fig. 1, it is observed that the height of the $\tan \delta$ peak of the EVA 26 is increased from 0.31 to 0.37 for the 0 and 2.0 phr DCP content, respectively, which suggests that the amorphous phase in the EVA increases when the EVA is crosslinked by the DCP.

Fig. 2 shows the X-ray diffraction patterns of the EVA 26 with DCP content. The X-ray patterns shown in Fig. 2 represent broad peaks than the crystalline polymer in general [9]. The broad peak may be caused by the reduction of the stereoregularity because of the VA in the EVA. For the EVA 26 containing 0.5, 1.0, 1.5 and 2.0 phr DCP, the X-ray diffraction patterns are shown to similar among the samples and the small peaks are observed at 9 and 28° which correspond the DCP [10]. For the EVA 26 without DCP, a low intensity

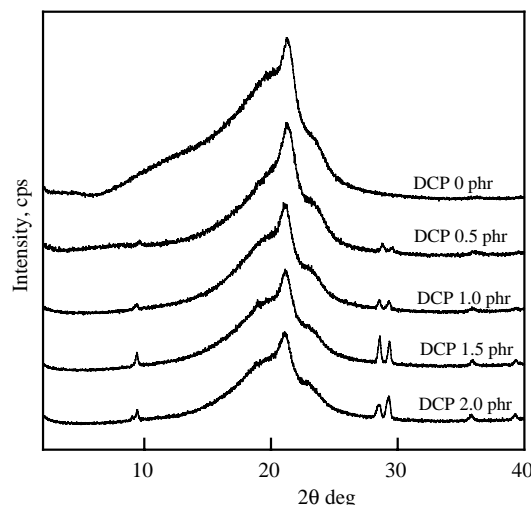


Fig. 2. X-ray diffraction patterns of the EVA 26 with DCP content.

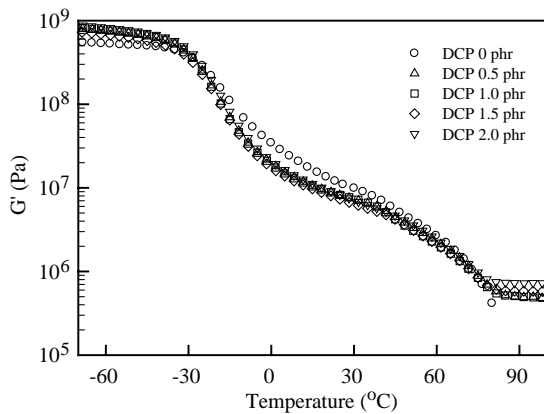


Fig. 3. Storage modulus (G') vs temperature for the EVA 26 with DCP content: (○) 0 phr DCP; (△) 0.5 phr DCP; (□) 1.0 phr DCP; (◇) 1.5 phr DCP; (▽) 2.0 phr DCP.

peak is observed between $2\theta = 10$ and 17° . From Fig. 2, it is observed that the shoulder between $2\theta = 10$ and 17° is disappeared by increasing the DCP content in the EVA 26.

Fig. 3 shows the storage modulus (G') vs temperature for the EVA 26 with DCP content. From Fig. 3, the storage modulus of the EVA 26 containing 0.5, 1.0, 1.5 and 2.0 phr DCP is observed to similar values among the samples. For the EVA 26 without DCP, the storage modulus between -20 and 30°C shows slightly higher value compared the EVA 26 with DCP. From the results of the $\tan \delta$ peak, X-ray diffraction pattern and storage modulus of the EVA 26, it is suggested that the storage modulus of the EVA 26 between -20 and 30°C may be influenced by the rigid amorphous fraction of the EVA [6,7].

Fig. 4 shows the complex viscosity (η^*) vs frequency for the EVA 26 with and without DCP at 130°C . The crystalline phase of the EVA 26 is completely melted at 130°C , therefore the EVA 26 becomes amorphous phase in the melt state. Many researchers have been studied the property-structure relationship by rheological measurements [11–18]. From Fig. 4, the complex viscosity of the EVA 26 containing 0.5, 1.0, 1.5

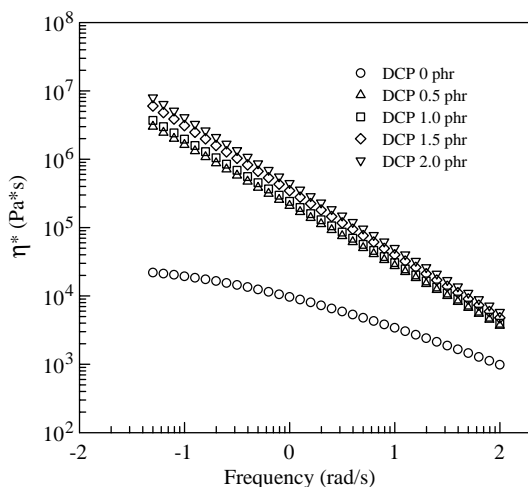


Fig. 4. Complex viscosity (η^*) vs frequency for the EVA 26 with and without DCP at 130°C : (○) 0 phr DCP; (△) 0.5 phr DCP; (□) 1.0 phr DCP; (◇) 1.5 phr DCP; (▽) 2.0 phr DCP.

Table 2
Power law parameter (n) of the EVA

Samples	DCP content (phr)				
	0.0	0.5	1.0	1.5	2.0
EVA 26	0.50	0.11	0.10	0.06	0.05
EVA 33	0.41	0.10	0.08	0.09	0.05
EVA 41	0.39	0.11	0.07	0.05	0.04
EVA 46	0.43	0.12	0.09	0.06	0.03

and 2.0 phr DCP is shown to increase at all frequencies compared EVA without DCP. From Fig. 4, it is observed that the increase of the complex viscosity of the EVA 26 is significant at the low frequencies (below 1 rad/s) for the EVA with DCP. To analyze crosslinking of the EVA with DCP qualitatively, the power-law relationship [19] is introduced:

$$\eta^* = m|\omega|^{n-1} \quad (1)$$

where ω is the frequency and η^* is the complex viscosity. The m and n are the fitting parameters.

In applying Eq. (1) to Fig. 4, we can find the slope of the η^* , which is $n-1$. The parameter $n-1$ corresponds the slope of the complex viscosity (η^*) in log–log plot which reflects the shear thinning behavior. Therefore, the decrease of the n represents the increase of crosslinking in the EVA. In general, the shear thinning is more pronounced in the solid like material such as crosslinked polymer and polymer composites [20]. From the results of the Eq. (1), it is obtained that the values of the power law parameter (n) are 0.50, 0.11, 0.10, 0.06 and 0.05 for the EVA 26 with 0.0, 0.5, 1.0, 1.5, and 2.0 phr DCP, respectively. From the results of the power law parameter (n) of the η^* which are shown in Table 2, it is suggested that the crosslinking of the EVA could be known by the values of the power law parameter (n).

3.2. Effects of VA content

Fig. 5 shows the loss factor ($\tan \delta$) vs temperature for EVA with VA content. For the EVA 26, EVA 33, EVA 41, and EVA 46, the maximum $\tan \delta$ peak is observed at -16°C . From Fig. 5, it is observed that the height of the $\tan \delta$ peak of

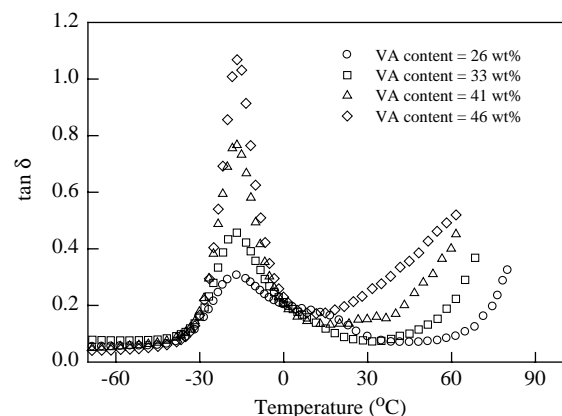


Fig. 5. Loss factor ($\tan \delta$) vs temperature for the EVA with VA content: (○) EVA 26; (□) EVA 33; (△) EVA 41; (◇) EVA 46.

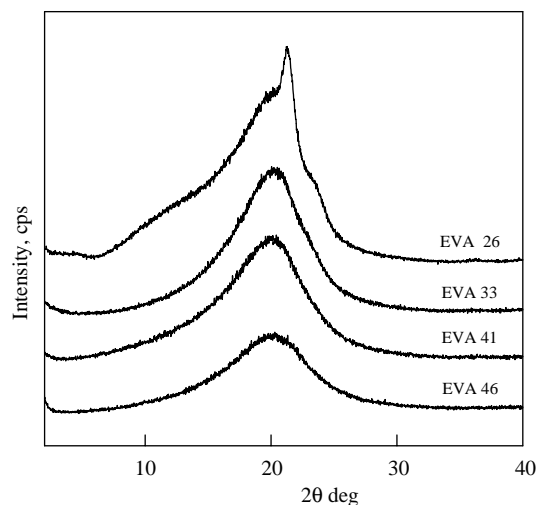


Fig. 6. X-ray diffraction patterns of the EVA with VA content.

the EVA 26, EVA 33, EVA 41, and EVA 46 is increased with increasing the VA content. The height of the $\tan \delta$ peak increases from 0.31 to 1.07 for the EVA 26 and EVA 46, respectively, which suggests that amorphous phase is increased with the increase of the VA content in the EVA.

Fig. 6 shows the X-ray diffraction patterns of the EVA with VA content. For the EVA 26, EVA 33, EVA 41, and EVA 46, the X-ray patterns of the EVA is observed to be broader with the increase of the VA content, which suggests that the crystallinity of the EVA decreases with the increase of the VA content.

Fig. 7 shows the storage modulus (G') vs temperature for the EVA with VA content. From Fig. 7, the storage modulus below -30°C which is below the glass transition temperature of the EVA is shown to be similar values among the samples. It has been reported that the storage modulus below the glass transition region can be hardly affected by changing the crystallinity of the polymer [21]. From Fig 7, the storage modulus above -30°C decreases with increasing the VA content. This result is consistent with the above results of the $\tan \delta$ and X-ray diffraction pattern that the crystallinity decreases with the increase of the VA content in the EVA. From the results of

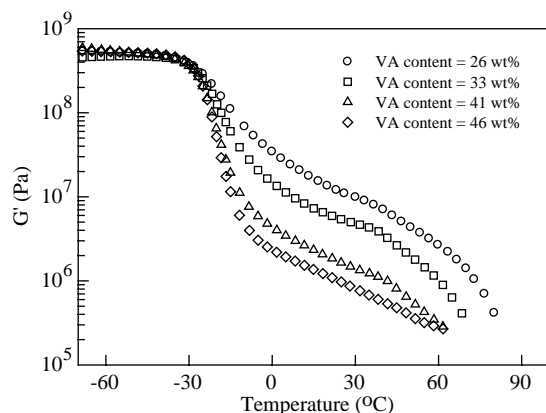


Fig. 7. Storage modulus (G') vs temperature for the EVA with VA content: (○) EVA 26; (□) EVA 33; (△) EVA 41; (◇) EVA 46.

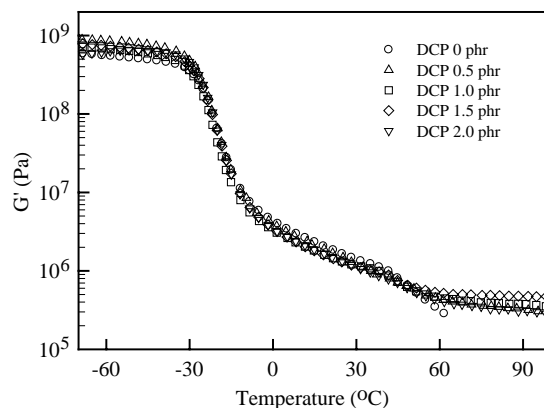


Fig. 8. Storage modulus (G') vs temperature for the EVA 41 with DCP content: (○) 0 phr DCP; (△) 0.5 phr DCP; (□) 1.0 phr DCP; (◇) 1.5 phr DCP; (▽) 2.0 phr DCP.

the $\tan \delta$ peak, X-ray diffraction patterns and storage modulus of the EVA with the VA content, it is suggested that the crystallinity of the EVA affects the storage modulus of the EVA above -30°C .

Fig. 8 shows the storage modulus (G') vs temperature for the EVA 41 with DCP content. From Fig. 8, the storage modulus of the EVA 41 containing the 0.0, 0.5, 1.0, 1.5 and 2.0 phr DCP is observed to be similar values among the samples in the solid temperature range (about -70 to 50°C). For the EVA 26 in Fig. 3, the storage modulus of the EVA 26 without DCP showed slightly higher value compared the EVA 26 with DCP between -20 and 30°C . Compared with the EVA 26, the structure of the EVA 41 without DCP has less crystallinity which can be seen in Figs. 5 and 6 such that the $\tan \delta$ shoulder and low intensity peak are not observed, respectively, which could be regarded as a rigid amorphous fraction of the EVA [6,7]. Therefore, the storage modulus of the EVA 41 with and without DCP showed the similar values among the samples, which suggests that the crosslinking of the EVA 41 has less effect on the storage modulus of the EVA. Considering the values of storage modulus of the EVA 26 and EVA 41 with and without DCP, the crosslinking of the EVA by DCP would be weak. From the above $\tan \delta$, X-ray diffraction patterns, and storage modulus of the EVA with VA content, it is suggested that the storage modulus in the solid temperature range (about -70 to 50°C) has the effect of the crystallinity of the EVA because of the weak crosslinking of the EVA by DCP.

In Table 2 shows the power law parameter (n) of the samples of EVA with VA content. From Table 2, the values of the power law parameter of the EVA without DCP ranged from 0.39 to 0.50 and the EVA with DCP ranged from 0.03 to 0.12. The decrease of the power law parameter of the EVA is observed at all EVA samples with DCP. In the measurement of complex viscosity of the EVA at the melt state, the crystal of the samples would melt, therefore, the crosslinking of the EVA could affect the complex viscosity of the EVA with DCP.

4. Conclusions

In this study, the effects of crosslinking and crystallinity on the thermal and rheological properties of the EVA were

investigated by dynamic mechanical thermal analysis, X-ray diffractometry and rheological measurements.

In the studies of the storage modulus of the EVA with VA content, the storage modulus above -30°C decreased with increasing the VA content. This result suggested that the crystallinity of the EVA affected the storage modulus of the EVA in the solid temperature range because of the weak crosslinking of the EVA by DCP.

From the results of the complex viscosity of the EVA in the melt state, the crosslinking of the EVA could be known by the values of the power law parameter (n). The values of the power law parameter (n) of the EVA without DCP ranged from 0.39 to 0.50 and the EVA with DCP ranged from 0.03 to 0.12.

From the above results of the storage modulus of the EVA in the solid state, the crystallinity of the EVA affects the storage modulus of the EVA with and without DCP. In the measurement of the complex viscosity of the EVA in the melt state, the crosslinking affects the complex viscosity of the EVA with DCP.

Acknowledgements

This study was supported by research grants from the Korea Science and Engineering Foundation (KOSEF) through the Applied Rheology Center (ARC), an official KOSEF-created engineering research center (ERC) at Korea University, Seoul, Korea.

References

- [1] Brogly M, Nardin M, Schultz J. *J Appl Polym Sci* 1997;64(10):1903–12.
- [2] Arsac A, Carrot C, Guillet J. *J Appl Polym Sci* 1999;74(11):2625–30.
- [3] Bistac S, Kunemann P, Schultz J. *Polymer* 1998;39(20):4875–81.
- [4] Gospodinova N, Zlatkov T, Terlemezyan L. *Polymer* 1998;39(12):2583–8.
- [5] Kim S, Shin B, Hong J, Cho W, Ha C. *Polymer* 2001;42(9):4073–80.
- [6] Lee HS, Kim WN. *Polymer* 1997;38(11):2657–63.
- [7] Chun YS, Han YS, Hyun JC, Kim WN. *Polymer* 2000;41(24):8717–20.
- [8] Tsagaropoulos G, Eisenberg A. *Macromolecules* 1995;28(18):6067–77.
- [9] Alamo RG, Blanco JA, Agarwal PK, Randall JC. *Macromolecules* 2003;36(5):1559–71.
- [10] Liao H, Wu C. *Polym Plast Technol Eng* 2003;42(1):1–16.
- [11] Peón J, Vega JF, Aroca M, Martínez-Salazar J. *Polymer* 2001;42(19):8093–101.
- [12] Vega JF, Santamaría A, Muñoz-Escalona A, Lafuente P. *Macromolecules* 1998;31(11):3639–47.
- [13] Shroff RN, Mavridis H. *Macromolecules* 1999;32(25):8454–64.
- [14] Wood-Adams P, Costeux S. *Macromolecules* 2001;34(18):6281–90.
- [15] Gramespacher H, Meissner J. *J Rheol* 1992;36(6):1127–41.
- [16] Friedrich C, Gleinzer W, Korat E, Maier D, Wesse J. *J Rheol* 1995;39(6):1411–25.
- [17] Riemann RE, Cantow HJ, Friedrich C. *Macromolecules* 1997;30(18):5476–84.
- [18] Sung YT, Han MS, Hyun JC, Kim WN, Lee HS. *Polymer* 2003;44(5):1681–7.
- [19] Carreau PJ, De Kee DCR, Chhabra RP. *Rheology of polymeric systems*. New York: Hanser/Gardner; 1997 [Chapter 2].
- [20] Larson RG. *The structure and rheology of complex fluids*. New York: Oxford; 1999 [Chapter 1].
- [21] Nielsen LE, Landal RF. *Mechanical properties of polymers and composites*. New York: Marcel Dekker, Inc.; 1994.